

Cross-Linking Behavior of Diskotic Side-Chain Polymers in Solution

Marcel W. C. P. Franse, Klaas te Nijenhuis,* Jan Groenewold, and Stephen J. Picken

Polymer Materials and Engineering, Faculty of Applied Sciences, Delft University of Technology, Julianalaan 136, 2628 BL Delft, The Netherlands

Received October 1, 2003; Revised Manuscript Received July 15, 2004

ABSTRACT: The cross-linking behavior for a series of solutions of closely related diskotic side-chain polymers, differing in the tails of the mesogens, has been studied. Solubility parameters are used to describe the driving force for the cross-linking behavior in these solutions. Complex formation enthalpies of the physical networks as determined by dynamic rheological measurements in combination with a statistical network model are relatively low. Moreover, with a statistical theory for equilibrium polymers, used by Cates and Candau for slightly similar systems, an average number of disks in a cross-link is calculated. Only two disks appear to be incorporated in the majority of cross-links, whereas most of the disks are in a free state.

Introduction

Since their development in the late 1970s, diskotic side-chain polymers have received increasing attention.¹ The mesomorphic behavior of the diskotic side-chain polymers can be tailored by modifying the architecture of the molecules. Structural variation of the disk, the spacer, or the polymer backbone can lead to a change in the temperature range of the mesophase formation as well as in the type of mesophase.^{2–4} The possibility to conduct electronic charge through self-organized columnar assemblies is one of the unique fields of application that motivates the study of diskotic side-chain polymers.^{5,6} Another area of application is the use of diskotic mesogens in compensation films for liquid crystal displays. The negative birefringence and the capability to immobilize the director make these materials very suitable to improve the performance of twisted nematic displays.⁷

The intermolecular attractive and repulsive forces operating in diskotic side-chain polymers are the consequence of an interplay between various types of noncovalent interactions. The forces and dynamics associated with these subtle interactions can be investigated more closely by studying the behavior of diskotic side-chain polymers in solution. A series of diskotic side-chain polymers were prepared by Kouwer, differing in the tails of the mesogens.^{8,9} The structural and dynamical properties of one of the diskotic side-chain polymers in a solution were extensively discussed in a previous paper.¹⁰ For that purpose, a combined rheological and network model study was performed. A minor increase in the calculated number of cross-links per unit volume occurred when the temperature was decreased, and the functionality was assumed to be constant. On the other hand, when the number of cross-links per unit volume was assumed constant, the calculated functionality increased only slightly when the temperature was lowered. In this paper, a comparison with other diskotic side-chain polymers in solution will be made to gain more insight into the cross-linking behavior of these systems. The differences in solubility are used to explain the structural differences between the physical net-

works of the various diskotic side-chain polymers. In addition, a statistical theory for equilibrium polymers is used to calculate average numbers of disks that are stacked together in the cross-links.

The network model we shall use is based on the statistical cross-linking model of Flory and Stockmayer.^{11–15} Stockmayer was the first to derive a relationship between the cross-linking index and the sol fraction for cross-linking of any functionality. But because of his rigorous exclusion of intramolecular cross-links in the sol fraction, he was hesitant to apply this beyond the gel point. Nevertheless, Flory demonstrated the possibility of modeling tetrafunctional cross-linking of polymer molecules with a monodisperse distribution of the molecular weights at and beyond the gel point. Much later, te Nijenhuis generalized the model to comply with cross-links of any functionality and a polydisperse distribution of the molecular weights.^{16–18} It has to be mentioned that there is much agreement between the results of the cross-linking process of high molecular weight polymer calculated with this model and those more specific presented in the literature (e.g., Charlesby et al.,^{19,20} Langley et al.,^{21–23} Graessley et al.,^{24,25} Šomvársky et al.,²⁶ and Peppas et al.^{27,28}). For a so-called accumulated Schulz–Flory distribution with $\bar{M}_w/\bar{M}_n \geq 2$ the relationship between the equilibrium shear modulus, G_e (determined with oscillatory rheological measurements), and the sol fraction, w_s , is found to be

$$G_e = \frac{2cRT}{\bar{M}_w}(2 - \alpha) \left\{ A \left((1 - w_s^{f/2}) \frac{f-2}{f} - \frac{1 - w_s}{B} \right) \right\} \quad (1)$$

where

$$A = \frac{\alpha - 2 + \sqrt{\alpha^2 + 4(1 - \alpha)/w_s}}{2(1 - \alpha)z} \quad \text{with} \quad z = 1 - w_s^{f/2-1} \quad (2)$$

and

* To whom correspondence should be addressed.

$$B = \frac{\frac{Az}{1 + Az} - \frac{Az(1 - \alpha)^2}{1 + Az(1 - \alpha)}}{\ln \frac{1 + Az}{1 + Az(1 - \alpha)}} \quad (3)$$

and where f is the functionality of the cross-links (i.e., the number of polymers leaving the cross-links), c is the mass concentration of polymer (kg/m³), R is the gas constant (J/(mol K)), T is the absolute temperature (K), \bar{M}_w is the weight-average molecular weight of the polymer molecules before cross-linking (kg/mol), and α is the monomer conversion during preparation of the polymer, which can be calculated from the polydispersity index ($D = \bar{M}_w/\bar{M}_n$, where \bar{M}_n is the number-average molecular weight (kg/mol)):

$$D = \frac{\alpha - 2}{\alpha} \ln(1 - \alpha) \quad (4)$$

An overview of the network parameters that can be obtained with the model is shown in Figure 1. In Figure 1, \bar{M}_c is the average molar mass between the cross-links and $\bar{\gamma}$ the average cross-linking index, i.e., the average number of cross-links per primary polymer molecule.

For the described molecular weight distribution, the weight-average cross-linking index, $\bar{\gamma}_w$, is found to be

$$\bar{\gamma}_w = \frac{(1 - 1/2\alpha)[\alpha - 2 + \sqrt{\alpha^2 + 4(1 - \alpha)/w_s}]}{(1 - \alpha)(1 - w_s^{1/2-1})} \quad (5)$$

This is an important parameter because it is directly proportional to the cross-link number density N_{cr} :

$$N_{cr} = \frac{2\bar{\gamma}_w}{f} \frac{cN_{Av}}{\bar{M}_w} \quad (6)$$

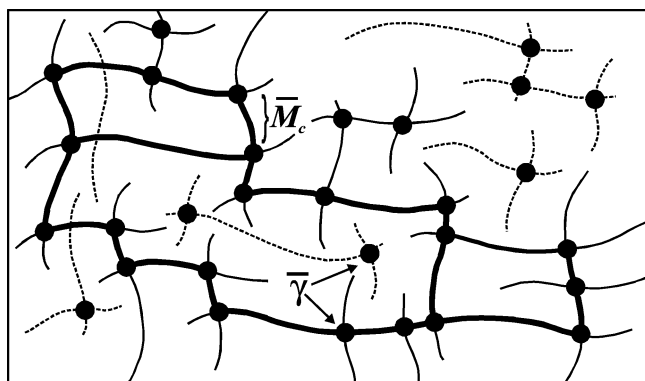
where N_{Av} is Avogadro's number.

Experimental Section

Materials. A series of liquid crystalline side-chain polymers bearing large disk-shaped mesogens with different tails ($\sim R$) were prepared by Kouwer (see Figure 2).^{8,9,29} The diskotic side-chain polymers were prepared through substitution of the mesogen on a reactive poly(acryloyl chloride).⁸ The number- and weight-average degrees of polymerization of the poly(acryloyl chloride), respectively 64 and 186, were determined by gel permeation chromatography. The degree of substitution of the active groups by the mesogen, x , was determined with nuclear magnetic resonance analysis. The remaining chloride atoms were substituted by methoxy groups. Figure 3 gives a schematic representation of the diskotic side-chain polymers. The solvent, 1,1,2-trichloroethane (bp 110 °C and $d_{20} = 1.43$ g/cm³), was purchased from Fisher Scientific. 11.0%, 9.0%, and 10.8% (w/w) solutions of the diskotic side-chain polymers with methyl, oxymethyl, and oxyhexyl ended mesogens, respectively, were prepared by weighing polymer and solvent. The polymers were dissolved by heating the solutions to 70 °C, gently stirring them in a closed vessel.

Equipment. The rheological experiments were conducted on a controlled strain Rheometrics Ares rheometer equipped with a Couette setup. The diameters of the bob and cup were 31.97 and 33.90 mm, respectively. The length of the bob was 33.35 mm. A minimum torque of 4 mg·cm could be measured, which corresponds to a shear stress of 7.3×10^{-3} N/m².

Measurements. Oscillatory measurements were carried out to study the rheological behavior of the diskotic side-chain polymer solutions and their relative differences. Between

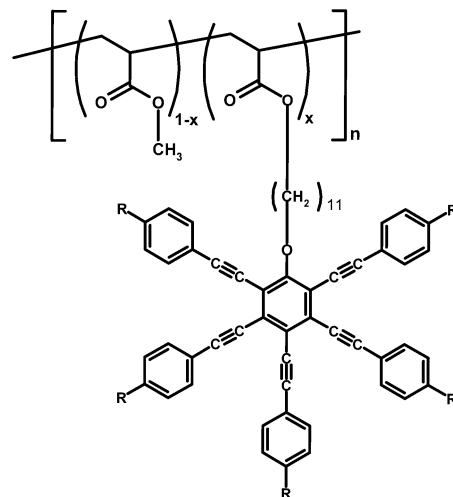


..... sol fraction w_s

_____ fraction of dangling ends w_f

_____ fraction of ideal network w_m

Figure 1. Schematic representation of a gel network.



$\sim R$	n	x
$\sim CH_3$	64	0.64
$\sim OCH_3$	64	0.83
$\sim OC_6H_{13}$	64	0.60

Figure 2. Chemical structure of the diskotic side-chain polymers.

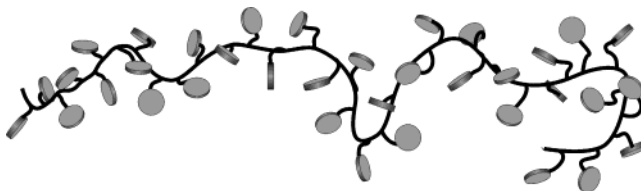


Figure 3. Schematic representation of the diskotic side-chain polymers.

successive series of measurements, the solution was allowed to rest for half an hour.

We found that the measurements could only be performed in a relative small temperature and concentration range.

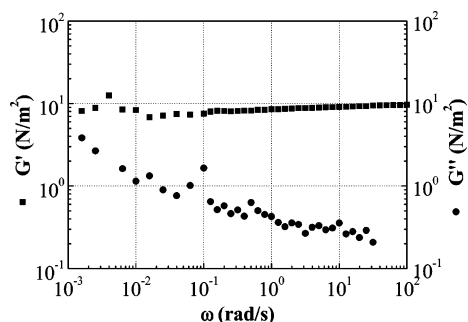


Figure 4. Dynamic frequency sweep experiments of a 13% (w/w) solution of diskotic side-chain polymer with methyl ended mesogens in 1,1,2-trichloroethane at 30 °C.

Phase separation occurred below certain temperatures or above a specific concentration, whereas no physical network was being formed and a regular solution of polymers existed above a specific temperature or below certain concentrations. The exact determination of the phase diagram turned out not to be possible due to the fact that the sol–gel transition was situated below the detection limit of the rheometer. However, useful measurements of a physical network were performed at a concentration range of 7–13% (w/w) of the polymer in trichloroethane. The measurement temperature was adjusted dependent on the concentration but was always between 6.6 and 40 °C.

Dichloromethane was used to recover the diskotic side-chain polymers. The dichloromethane and remaining 1,1,2-trichloroethane were removed under reduced pressure.

Results

A dynamic frequency sweep of a 13% (w/w) solution of the diskotic side-chain polymer with the methyl ended mesogens, in the linear viscoelastic region, is shown in Figure 4.

The curve of the storage modulus (G') as a function of frequency shows a rubber plateau over at least 5 decades. This rubber plateau indicates that a network of cross-linked polymer molecules might be present in the system. This hypothesis is further confirmed by considering the curve of the loss modulus (G'') also. In the whole measured frequency range the loss modulus is smaller than the storage modulus, as would have been expected for a network in its rubbery state.³⁰ Moreover, the increase of the loss modulus with decreasing frequency indicates the homogeneous nature of the system. Clearly, an increase in the loss modulus with decreasing frequency must be succeeded by a decrease at lower frequencies, i.e., at longer times (everything flows: Deborah). The homogeneous nature of a dynamic physical network is demonstrated by this prominent relaxation process. Unfortunately, the transitions for the dynamic physical network from rubberlike to glasslike behavior at high frequencies and from rubberlike to liquidlike behavior at low frequencies fall outside the range of the measurements.^{31,32}

The temperature dependence of the rubber plateau for a 9% (w/w) solution of the diskotic side-chain polymers with the methyl ended mesogens is shown in Figure 5. According to the previous discussion, the decrease in the absolute value of the rubber plateau is caused by a decrease in the number of cross-links. More rheological measurements are discussed in a previous paper.¹⁰

Discussion

In this discussion various analysis are combined in order to get a better idea about the cross-linking

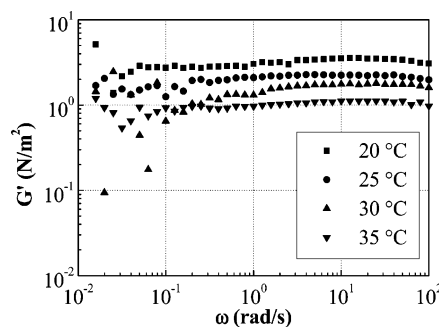


Figure 5. Dynamic frequency sweep experiments of a 9% (w/w) solution of diskotic side-chain polymer with methyl ended mesogens in 1,1,2-trichloroethane at 20, 25, 30, and 35 °C.

behavior and the structure of the cross-links in the system.

Solubility of the Diskotic Side-Chain Polymers.

Instead of trying to determine a value for every type of interaction in the solutions of the diskotic side-chain polymers, in this paper the cross-linking behavior will be approached at first more generally using solubility parameters; i.e., the incompatibility of the mesogen and the solvent is taken as the driving force for the cross-linking process.

Hildebrand defined the solubility parameter, δ , of a substance as the square root of the cohesive energy, E_{coh} , per unit of volume:³³

$$\delta = \left(\frac{E_{\text{coh}}}{V} \right)^{1/2} \quad (7)$$

The cohesive energy of a substance in a condensed state is defined as the energy needed per mole of substance to eliminate all intermolecular forces. In a refined theory not only dispersion forces but also polar forces and hydrogen bridge formations between the molecules are taken into account:³⁴

$$\delta_{\text{tot}}^2 = \delta_d^2 + \delta_p^2 + \delta_h^2 \quad (8)$$

where δ_d is the solubility parameter contribution of dispersion forces, δ_p the solubility parameter contribution of polar forces, and δ_h the solubility parameter contribution of hydrogen bonding. In addition, the contributions of polar forces and hydrogen bridge formations are corrected for the presence of symmetry planes. The different contributions are determined from the group contributions of molecular parts presented in the literature.³⁴

The solubility of a given polymer is primarily determined by its chemical structure. As a general rule, structural similarity favors solubility. Consequently, for a substance to be soluble in a solvent the various contributions of the solubility parameter of the polymer and the solvent may not differ too much. As a general rule³³

$$\Delta\delta^2 = (\delta_{ds} - \delta_{dp})^2 + (\delta_{ps} - \delta_{pp})^2 + (\delta_{hs} - \delta_{hp})^2 \leq 45 \text{ J/cm}^3 \quad (9)$$

for a polymer (p) with a substitution degree of 64 to be soluble in the solvent (s). For the smaller mesogen this value is around 75. For the calculation of the various contributions to the solubility parameters, data were taken from the book by van Krevelen.³⁴ The results are given in Table 1. The differences in solubility param-

Table 1. Solubility Parameters Contributions of the Diskotic Side-Chain Polymers

	solvent	mesogen			polymer backbone
		$\sim\text{CH}_3$	$\sim\text{OCH}_3$	$\sim\text{OC}_6\text{H}_{13}$	
δ_d ($\text{J}^{1/2}/\text{cm}^{3/2}$)	20.9	22.4	21.8	19.7	20.7
δ_p ($\text{J}^{1/2}/\text{cm}^{3/2}$)	5.84	0.38	0.75	0.47	6.81
δ_h ($\text{J}^{1/2}/\text{cm}^{3/2}$)	3.84	2.17	5.15	4.07	8.86
δ_{tot} ($\text{J}^{1/2}/\text{cm}^{3/2}$)	22.0	22.6	22.4	20.2	23.5

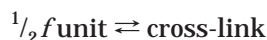
eters according to eq 9 are for the polymer backbone with the solvent and the mesogens with the solvent given in Table 2. It is clear that the differences in the solubility parameters of the polymer backbone and the solvent or the mesogens and the solvent are within the limit set in eq 9. Moreover, the difference with solvent is smaller for the polymer backbone compared to those of the mesogens.

Accordingly, the cross-links in the physical network are most probably formed by the aggregation of the mesogens.

Also notable is the trend in $\Delta\delta^2$ of the mesogens and the solvent. The difference increases in the order of the systems with mesogens with the oxymethyl, the oxyhexyl, and the methyl tails. A closer look at the various contributions of the solubility parameters reveals more insight into this order. In this study, the most important features of the chemical structure of the solvent molecules are the presence of chloride atoms and their relatively high density. The chloride groups give the solvent molecules polar and hydrogen-bonding capabilities. The mesogens, on the other hand, contain a relatively low number of groups that exert polar forces. It is these contributions, or better the lack of them, that is responsible for the major part of the solubility parameters. The introduction of an oxygen atom in the tails of the mesogens is expected to cause an increase in the polar nature as well as the capability of hydrogen bonding. Indeed, this effect is clearly visible upon comparing the solubility parameter contributions of the mesogens with the methyl and the oxymethyl tails. The polar contribution of the oxygen atom is partly canceled out if subsequently the oxymethyl tails are replaced by the oxyhexyl tails, as is seen in Table 1. The total solubility parameter of the mesogens with the oxyhexyl tails and the solvent is between the total solubility parameter of the other types of mesogens.

Determination of the Complex Formation Enthalpies. The cross-linking behavior of the various solutions of the diskotic side-chain polymers can also be compared through calculation of the formation enthalpy of the cross-links. In addition, a relative comparison can be made to more familiar systems such as the cross-link formation by hydrogen bonds.

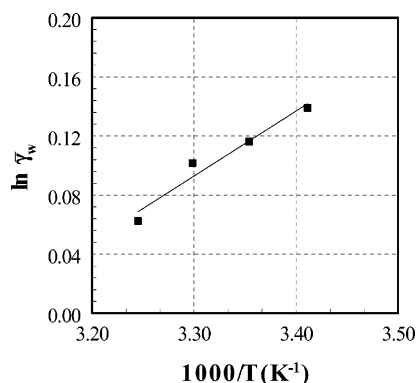
The formation enthalpy of a cross-link can be determined as follows. The equilibrium of the cross-linking process for a reversible physical network can be defined as



where f is the functionality of the cross-link. Subsequently, the equilibrium constant, K , can be defined as

$$K = \frac{[\text{cross-link}]}{[\text{unit}]^{f/2}} = K^0 \exp(-\Delta H/RT) \quad (10)$$

where ΔH is the formation enthalpy of 1 mol of cross-

**Figure 6.** Natural logarithm of $\bar{\gamma}_w$ as a function of $1/T$ for a 9% (w/w) solution of diskotic side-chain polymers with methyl ended mesogens in 1,1,2-trichloroethane, calculated for $f = 4$.**Table 2. Solubility Parameters Differences with Respect to the Solvent**

	mesogen			polymer backbone
	$\sim\text{CH}_3$	$\sim\text{OCH}_3$	$\sim\text{OC}_6\text{H}_{13}$	
$\Delta\delta^2$ (J/cm^3)	35.1	28.5	30.2	26.2

Table 3. Formation Enthalpies of Cross-Links in Solutions of the Diskotic Side-Chain Polymers in 1,1,2-Trichloroethane¹⁰

$\sim\text{R}$	ΔH (kJ/mol)
$\sim\text{CH}_3$	-4.1 ± 0.5
$\sim\text{OCH}_3$	-1.4 ± 0.3
$\sim\text{OC}_6\text{H}_{13}$	-2.6 ± 0.3

links. The concentration of cross-links is directly proportional to weight-average cross-linking index, $\bar{\gamma}_w$. Hence, the slope of a curve of $\ln(\bar{\gamma}_w)$ vs $1/T$ is equal to $\Delta H/R$, provided the number of potential cross-link units is much larger than is actually used in cross-links:

$$\ln \bar{\gamma}_w = \ln K^0 - \Delta H/RT \quad (11)$$

This is definitely the case because the number of cross-links per primary polymer molecule is only slightly above 1.¹⁰ The weight-average cross-linking index can be calculated with eqs 1–5.

Figures 5 and 6 show such a measurement for a 9% (w/w) solution of the diskotic side-chain polymers with the methyl ended mesogens.

Table 3 shows the results for all the various solutions of diskotic side-chain polymers, where the functionality was assumed to be 4.

The calculated values of the cross-link formation enthalpy are relatively low, for a functionality of 4. In comparison, a hydrogen bridge has on average a formation enthalpy of -21 kJ/mol. The values of ΔH increase slightly when the same calculations are performed assuming a higher functionality of the cross-links. However, they remain low, even upon assuming an improbably high functionality of 20; the highest calculated formation enthalpy of the diskotic side-chain polymers with the methyl ended mesogens is only -11.4 kJ/mol.

Besides by an increase in the number of cross-links, the equilibrium shear modulus of a network also increases when more polymer molecules are joined in the same number of cross-links. Cross-linking can then be compared with a secondary nucleation process.³¹ Hence, instead of the functionality of the cross-links, also the number of cross-links per unit volume can be

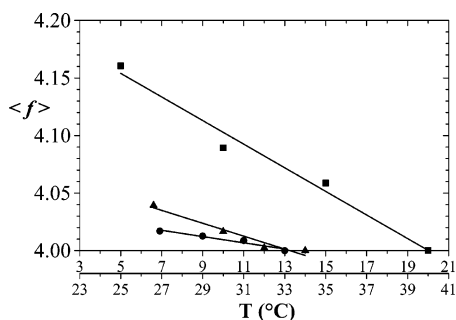


Figure 7. Average functionality of the cross-links as a function of the temperature at a constant value of the number of cross-links per unit volume in diskotic side-chain polymer solutions for mesogens with methyl tails (squares and lower x -axis), oxymethyl tails (circles and upper x -axis), and oxyhexyl tails (triangles and upper x -axis) (starting with $f_0 = 4$).

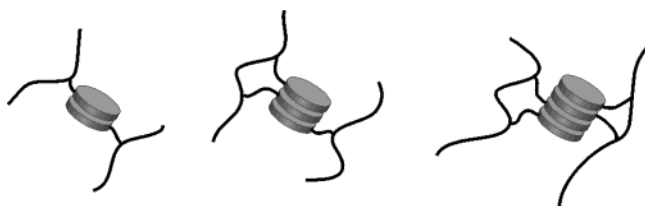


Figure 8. Schematic representation of various cross-links with cross-link functionality 4, with $L = 2, 3$, and 4.

assumed to be constant. In that case, the dependence of the functionality upon the temperature can be determined. In Figure 7, the cross-link functionality is plotted as a function of the temperature at a constant cross-link density, N_{cr} , for the three different systems. Therefore, the cross-link density at the highest temperature is taken as a reference point. Calculations were performed for a starting point of the functionality $f_0 = 4$.

Only a small increase in the average functionality of the cross-links as a function of decreasing temperature is observed in Figure 7. The increase of the functionality for a temperature decrease of 15 °C is at most 3%. However, this increase becomes larger when at first a higher functionality of the cross-links is assumed. For example, when the functionality is assumed to be 16, the maximum increase over the same temperature range becomes 12%.¹⁰ The functionality shows a larger relative increase for the same decrease in temperature for the systems with the oxymethyl, oxyhexyl, and methyl tails in the mesogens.

Calculation of the Number of Disks Incorporated in a Cross-Link. Although for the calculation of the complex formation enthalpies the cross-link functionality was assumed to be 4, the number of disks that are present in those cross-links could still vary (see Figure 8). The complex formation enthalpies calculated from the equilibrium shear modulus can be used to gain more insight into the number of disks that are incorporated in a cross-link.

For that purpose, we made use of a relationship for the average stacking number of disks, $\langle L \rangle$, that was used by Cates and Candau to calculate an average chain length of wormlike micelles in surfactant solutions.³⁵ Already in 1965, Scott derived similar relationships to calculate an average chain length of open-chain sulfur (S_n) in nonelectrolyte solvents.³⁶ For an ensemble of linear chains of stacked disks in a solvent, inscribed for convenience on a unit lattice, the relevant terms, in

relation to the number of stacked disks in a chain, are¹⁵

$$\frac{F}{RT} = \sum_L C(L) \left[\ln C(L) + \frac{E}{RT} \right] \quad (12)$$

where F is the free energy per unit volume, $C(L)$ the number density of stacks with L disks, and E the energy needed to separate one disk from a stack. For a cross-link functionality of 4 and a low number of disks stacked together in a cross-link, this energy E can be assumed to correspond closely to the complex formation enthalpy, ΔH (see Table 3). The origin of the entropy term is a combinatorial one: In how many ways can we form a particular distribution of stack sizes? The influence of connectivity on such an entropy is minor, although some modification can be expected: (1) modified intrachain association for two neighboring disks on a chain because these interactions are strongly modified by the backbone; (2) diminished association for next-nearest-neighboring disks and intrachain interactions beyond next-nearest neighbors. A number of disks are unable to associate due to the persistence of the chain. (So, the number of unavailable disks is proportional to the persistence length.) We do not need to consider intrachain interactions beyond that, as these are statistically indistinguishable from interchain interactions. The first effect manifests itself as a slight modification of the stacking energy, E . The second effect is negligible because the overwhelming majority of combinations stem from interchain interactions or from intrachain interactions of two neighboring disks. To proceed, we must fix the total volume fraction of disks:³⁵

$$\phi_m = \sum_L LC(L) \quad (13)$$

The first term of the right-hand side of eq 12 is the entropy contribution of the chain where the part of the free energy that is extensive in the chain length has been set to zero, as we are only interested in the minimum free energy as a function of chain length. The term, originating from the entropic contributions of the solvent and the mean-field interaction, can be omitted for the same reason. Equation 12 can now easily be minimized by addition of the constraint (13) with a Lagrange multiplier, yielding³⁵

$$C(L) = \frac{\phi_m}{\langle L \rangle^2} \exp\left(-\frac{L}{\langle L \rangle}\right) \quad (14)$$

and

$$\langle L \rangle = \phi_m^{1/2} \exp\left(\frac{1}{2} + \frac{E}{2RT}\right) \quad (15)$$

Equation 15 indicates that an increase in the concentration of disks causes an increase of the number of disks that are stacked together in a cross-link. Raising the temperature, on the other hand, has an opposite effect. The second column in Table 4 gives an overview of the calculated average chain lengths of stacked disks for the various diskotic side-chain polymers in 1,1,2-trichloroethane.

The last column will be referred to later on.

For all three cases, the average chain length is around 1. Equations 14 and 15 are derived for systems with long stacks ($L \gg 1$) as in linear micelles. Apparently, our system is not completely appropriate for these

Table 4. Average Stacking Lengths of the Number of Disks, Calculated from Eqs 15 and 17

$\sim R^a$	$\langle L \rangle$ (eq 15)	$\langle L \rangle$ (eq 17)
$\sim CH_3$	1.37	1.95
$\sim OCH_3$	0.75	1.40
$\sim OC_6H_{13}$	1.06	1.65

^a $\sim R$ indicates the end groups of the mesogen.

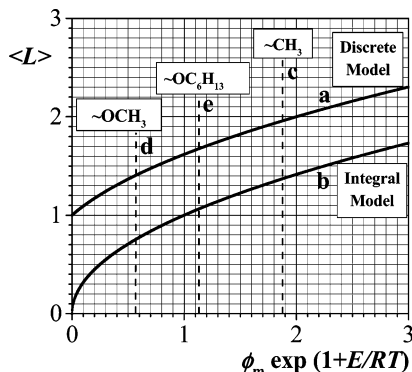


Figure 9. Average disk chain length for (a) the discrete and (b) the integral model as a function of $\phi_m \exp(1 + E/RT)$. The vertical dashed lines indicate the appropriate values for the various solutions of the diskotic side-chain polymers with (c) $\sim CH_3$ ended mesogens, (d) $\sim OCH_3$ ended mesogens, and (e) $\sim OC_6H_{13}$ ended mesogens.

equations. For the derivation of eqs 14 and 15, L was allowed to vary continuously. At these low values of $\langle L \rangle$, however, we have to take a discrete approach. For summations starting at $L = 1$ the results then become

$$C(L) = \frac{\phi_m}{\langle L \rangle^2 - \langle L \rangle} \left(\frac{\langle L \rangle - 1}{\langle L \rangle} \right)^L \quad (16)$$

and

$$\langle L \rangle = \frac{1}{2} + \frac{1}{2} \sqrt{1 + 4\phi_m \exp\left(1 + \frac{E}{RT}\right)} \quad (17)$$

The results of eqs 16 and 17 approach those of eqs 14 and 15, respectively, for large values of $\langle L \rangle$. For low values of $\langle L \rangle$ the difference becomes more eminent, and the discrete model is preferred. Figure 9 gives an overview of the two models. The x -axis has been chosen to accommodate the various systems.

The last column in Table 4 gives an overview of the newly calculated average numbers of stacked disks. The average values of the number of stacked disks are now between 1 and 2. The oxymethyl ended mesogens have the lowest average value, in agreement with the calculated complex formation enthalpies.

Table 5 gives an overview of the various number densities of stacked disks, $C(L)$. They are plotted as a function of the number of disks in a complex, L , in Figure 10. In addition, the relative fractions of the complexes are also given in Table 5. Therefore, the total amount of complexes ($\sum C(L)$) is given by

$$\sum_{L=1}^{\infty} C(L) = \frac{\phi}{\langle L \rangle} \quad (18)$$

The majority of the disks are in a free state. This was expected because of the relatively low formation enthalpies in Table 3. For every system about a quarter of the number of disks belong to a complex of two disks. The

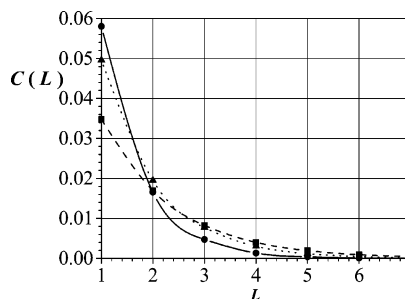


Figure 10. Number densities of the various complexes. The lines are drawn to guide the eye. The squares represent the methyl ended mesogens, the circles the oxymethyl ended mesogens, and the triangles the oxyhexyl ended mesogens.

Table 5. Various Fractions of Stacked Disks

$\langle L \rangle$	$\sim CH_3$		$\sim OCH_3$		$\sim OC_6H_{13}$	
	$C(L)$	fraction	$C(L)$	fraction	$C(L)$	fraction
1	0.035	0.51	0.058	0.71	0.050	0.61
2	0.017	0.25	0.017	0.20	0.020	0.24
3	0.008	0.12	0.005	0.06	0.008	0.09
4	0.004	0.06	0.001	0.02	0.003	0.04
5	0.002	0.03			0.001	0.02

assumption that the energy E is corresponding to the complex formation enthalpy appears to be a valid one. A small fraction of disks is incorporated into stacks of three disks.

Figure 10 clearly indicates the steep drop in $C(L)$ for values of L larger than 1.

In addition, no long-range ordering could be measured by X-ray measurements of a 9% (w/w) solution of the diskotic side-chain polymer with methyl ended mesogens.³⁷ As such, the assumption of a constant functionality of 4 for the cross-links in the calculation of the complex formation enthalpies is consistent with these results.

Not all disks that are incorporated in a complex form a cross-link between two polymers. The various disks in a complex can originate from the same polymer. For the diskotic side-chain polymers with the methyl ended mesogens there are on average 37 disks not in a free state. From the rheological measurements, we were able to determine that a polymer molecule is on average 1.1 times cross-linked to another polymer molecule.¹⁰ This indicates that the majority of disks are connected to a disk that belongs to the same molecule.

Conclusions

The use of solubility parameters appears to be a good tool to predict the cross-linking behavior of our diskotic side-chain polymers in 1,1,2-trichloroethane. Using dynamic rheological measurements, the presence of a physical network in solutions of diskotic side-chain polymers with mesogen with a methyl, oxymethyl, or oxyhexyl tail was demonstrated. In all cases, a relatively low complex formation enthalpy was measured. From the calculation of the average stacking lengths of disks with a statistical theory for equilibrium polymers, it appeared that the majority of the mesogens are in a free state. Most of the present cross-links are composed of two disks, and only a small fraction contain three or four disks. The presence of cross-links with a higher number of disks is negligible.

Acknowledgment. The authors gratefully acknowledge Dr. P. H. J. Kouwer for the synthesis of the diskotic

side-chain polymer. We thank Mr. B. Norder and Mr. G. de Vos for technical assistance. The support of the Dutch Polymer Institute (Dr. J. Groenewold) is gratefully acknowledged.

References and Notes

- (1) Kreuder, W.; Ringsdorf, H. *Makromol. Chem., Rapid Commun.* **1983**, *4*, 807.
- (2) Janietz, D.; Praefcke, K.; Singer, D. *Liq. Cryst.* **1993**, *13*, 247.
- (3) Keinan, E.; Kumar, S.; Singh, S. P.; Ghirlando, R.; Wachtel, E. *J. Liq. Cryst.* **1992**, *11*, 157.
- (4) Zamir, S.; Singer, D.; Spielberg, N.; Wachtel, E. J.; Zimmermann, H.; Poupko, R.; Luz, Z. *Liq. Cryst.* **1996**, *21*, 39.
- (5) van de Craats, A. M.; Warman, J. M.; de Haas, M. P.; Adam, D.; Simmerer, J.; Haarer, D.; Schuhmacher, P. *Adv. Mater.* **1996**, *8*, 823.
- (6) Karthaus, O.; Ringsdorf, H.; Tsukruk, V. V.; Wendorff, J. H. *Langmuir* **1992**, *8*, 2279.
- (7) Sergan, T. A.; Jamal, S. H.; Kelly, J. R. *Displays* **1999**, *20*, 259.
- (8) Kouwer, P. H. J.; Jager, W. F.; Mijs, W. J. *Macromolecules* **2000**, *33*, 4336.
- (9) Kouwer, P. H. J. In *Doctoral Thesis*, Delft University of Technology, 2002.
- (10) Franse, M. W. C. P.; te Nijenhuis, K.; Picken, S. J. *Rheol. Acta* **2003**, *42*, 443.
- (11) Flory, P. J. *J. Am. Chem. Soc.* **1941**, *63*, 3096.
- (12) Flory, P. J. *J. Am. Chem. Soc.* **1947**, *69*, 30.
- (13) Stockmayer, W. H. *J. Chem. Phys.* **1943**, *2*, 45.
- (14) Stockmayer, W. H. *J. Chem. Phys.* **1944**, *4*, 125.
- (15) Flory, P. J. *Principles of Polymer Chemistry*, 2nd ed.; Cornell University Press: Ithaca, NY, 1953.
- (16) te Nijenhuis, K. *Polym. Gels Networks* **1993**, *1*, 185.
- (17) te Nijenhuis, K. *Makromol. Chem.* **1991**, *192*, 603.
- (18) Franse, M. W. C. P.; te Nijenhuis, K. *Macromol. Theory Simul.* **2002**, *11*, 342.
- (19) Charlesby, A. *Proc. R. Soc. London* **1954**, *A222*, 542.
- (20) Charlesby, A.; Pinner, S. H. *Proc. R. Soc. London* **1959**, *A249*, 367.
- (21) Langley, N. R.; Ferry, J. D. *Macromolecules* **1968**, *1*, 353.
- (22) Langley, N. R.; Polmanteer, K. E. *Macromolecules* **1968**, *1*, 348.
- (23) Langley, N. R.; Polmanteer, K. E. *J. Polym. Sci., Polym. Phys. Ed.* **1974**, *12*, 1023.
- (24) Pearson, D. S.; Graessley, W. W. *Macromolecules* **1978**, *11*, 528.
- (25) Dossin, L. M.; Graessley, W. W. *Macromolecules* **1979**, *12*, 123.
- (26) Šomvársky, J.; te Nijenhuis, K.; Ilavský, M. *Macromolecules* **2000**, *33*, 3659.
- (27) Patterson, K. G.; Padgett, S. J.; Peppas, N. A. *Colloid Polym. Sci.* **1982**, *260*, 851.
- (28) Peppas, N. A.; Bures, P.; Leobandung, W. I. H. *Eur. J. Pharmacol. Biopharm.* **2000**, *50*, 27.
- (29) Kouwer, P. H. J.; Jager, W. F.; Mijs, W. J.; Picken, S. J. *Macromolecules* **2001**, *34*, 7582.
- (30) Winter, H. H.; Chambon, F. *J. Rheol.* **1986**, *30*, 367.
- (31) te Nijenhuis, K. *Polym. Gels Networks* **1996**, *4*, 415.
- (32) te Nijenhuis, K. In *Ph.D. Thesis*, Delft University of Technology, Delft, 1979; p 187.
- (33) Hildebrand, J. H.; Scott, R. L. *The Solubility of Non-Electrolytes*, 2nd ed.; Reinhold: New York, 1936.
- (34) van Krevelen, D. W. *Properties of Polymers*, 3rd ed.; Elsevier Science B.V.: Amsterdam, 1997.
- (35) Cates, M. E.; Candau, S. J. *J. Phys.: Condens. Matter* **1990**, *2*, 6869.
- (36) Scott, R. L. *J. Phys. Chem.* **1965**, *69*, 261.
- (37) Kouwer, P. H. J., private communication.

MA0354804